Muon $g-2$, rare kaon decays, and parity violation from dark bosons

Hooman Davoudiasl,[1] Hye-Sung Lee,[2,3] and William J. Marciano[1]

[1]*Department of Physics, Brookhaven National Laboratory, Upton, New York 11973, USA*
[2]*Department of Physics, College of William and Mary, Williamsburg, Virginia 23187, USA*
[3]*Theory Center, Jefferson Lab, Newport News, Virginia 23606, USA*

(Received 21 February 2014; published 8 May 2014)

The muon $g_\mu - 2$ discrepancy between theory and experiment may be explained by a light vector boson Z_d that couples to the electromagnetic current via kinetic mixing with the photon. We illustrate how the existing electron $g_e - 2$, pion Dalitz decay, and other direct production data disfavor that explanation if the Z_d mainly decays into $e^+e^-, \mu^+\mu^-$. Implications of a dominant invisible Z_d decay channel, such as light dark matter, along with the resulting strong bounds from the rare $K \to \pi +$ missing energy decay are examined. The K decay constraints may be relaxed if destructive interference effects due to $Z - Z_d$ mass mixing are included. In that scenario, we show that accommodating the $g_\mu - 2$ data through relaxation of K decay constraints leads to interesting signals for dark parity violation. As an illustration, we examine the alteration of the weak mixing angle running at low Q^2, which can be potentially observable in polarized electron scattering or atomic physics experiments.

DOI: 10.1103/PhysRevD.89.095006 PACS numbers: 14.70.Pw, 11.30.Er

I. INTRODUCTION

Dark matter constitutes about 22% of the Universe's energy-matter budget [1]. However, its exact nature remains elusive. Various speculative ideas have been proposed based on cosmologically stable candidate particles ranging in mass from below 1 GeV to above 1 TeV. Beyond gravity, dark matter interactions and other properties such as spin and extended spectroscopy are also uncertain, with conflicting evidence coming from sensitive underground experiments and astrophysical measurements.

An interesting generic property of some dark matter scenarios is the existence of a broken $U(1)_d$ gauge symmetry in the dark particle sector. Originally introduced to explain various astrophysics anomalies such as high-energy positron excesses or 511-keV photons originating from the galactic center [2], it has also been used to provide a novel explanation [3,4] for the 3.6σ discrepancy between the muon's experimental anomalous magnetic moment, $a_\mu \equiv (g_\mu - 2)/2$, and the Standard Model (SM) prediction. Employing the $U(1)_d$ gauge symmetry to accommodate this discrepancy is the guiding focus of this paper. In the simplest scenario, the low-mass $U(1)_d$ gauge boson known as the dark photon (or dark Z), Z_d, interacts with the SM particles via kinetic mixing with the photon, parametrized by $\varepsilon \ll 1$.

Existing experimental constraints on ε as a function of m_{Z_d} are reviewed and updated in Sec. II. There we discuss the region of parameter space favored by the discrepancy between measured and predicted values of a_μ as well as the bound (roughly $m_{Z_d} \gtrsim 20$ MeV) that follows from a comparison of experiment and theory for the electron anomalous magnetic moment. Bounds from $\pi^0 \to \gamma Z_d$ searches in Dalitz decays, $\pi^0 \to \gamma e^+e^-$, and direct Z_d production in electron scattering are also displayed.

Except for a_μ and a_e, most dark photon constraints assume $\mathrm{BR}(Z_d \to e^+e^-) \simeq 1$ for $m_{Z_d} < 2m_\mu$ [5]. Those bounds can be significantly relaxed if instead light "dark" particles exist with masses less than $m_{Z_d}/2$ and dominate the branching fractions via $Z_d \to$ invisible decays [6,7]. However, as we describe in Sec. III, the decay $K^+ \to \pi^+ +$ missing energy constraints then apply and continue to rule out large parts of the dark photon parameter space favored by the $g_\mu - 2$ discrepancy. In particular, the regions around $m_{Z_d} \sim 100$ and 200 MeV are already severely constrained.

In addition to the $K^\pm \to \pi^\pm Z_d$ loop-induced amplitude that arises from kinetic mixing, an amplitude of potentially similar magnitude can also arise from $Z - Z_d$ mass matrix mixing. We briefly review the latter formalism in Sec. IV. If destructive interference between the two amplitudes occurs, the $K^\pm \to \pi^\pm Z_d$ bound can be significantly relaxed, as shown in Sec. V. Such a cancellation requires a relationship between ε and the size of mass matrix mixing parametrized by a small-quantity ε_Z. We describe in Sec. VI how that relation leads to interesting definite predictions (dark parity violation) that are potentially observable at low Q^2 in the running of $\sin^2\theta_W(Q^2)$, where θ_W is the weak mixing angle. Finally, in Sec. VII, we present our conclusions.

II. THE STATUS OF DARK PHOTON SEARCHES

The interaction of a dark photon Z_d corresponding to a broken $U(1)_d$ gauge symmetry in the dark particle sector with the SM is induced by $U(1)_Y$ and $U(1)_d$ kinetic mixing [8] in the Lagrangian

$$\mathcal{L}_{\text{gauge}} = -\frac{1}{4}B_{\mu\nu}B^{\mu\nu} + \frac{1}{2}\frac{\varepsilon}{\cos\theta_W}B_{\mu\nu}D^{\mu\nu} - \frac{1}{4}D_{\mu\nu}D^{\mu\nu}, \quad (1)$$

where

$$B_{\mu\nu} = \partial_\mu B_\nu - \partial_\nu B_\mu, \qquad D_{\mu\nu} = \partial_\mu Z_{d\nu} - \partial_\nu Z_{d\mu} \tag{2}$$

and $|\varepsilon| \lesssim 10^{-2}$ is a (potentially loop-induced) mixing parameter. It can be viewed as an effective counterterm whose value is to be determined experimentally or in some models may be finite and calculable.

After field redefinitions employed to eliminate the cross term in Eq. (1), a coupling of the dark photon to the ordinary electromagnetic current is induced.

$$\mathcal{L}_{\text{dark}\,\gamma} = -\varepsilon e J^\mu_{em} Z_{d\mu}, \qquad J^\mu_{em} \equiv Q_f \bar{f}\gamma^\mu f + \cdots, \tag{3}$$

where Q_f is the electric charge of a given fermion f and the ellipsis represents nonfermionic currents. At leading order, the effective coupling is basically given by the $\gamma - Z_d$ mixing parametrized by ε. Since $|\varepsilon|$ is very small, the next-to-leading order ε^2 as well as $\mathcal{O}(\varepsilon m^2_{Z_d}/m^2_Z)$ effects can be neglected in the phenomenology we consider in this paper.

An attractive feature of the dark photon model is that there are only two parameters in its phenomenological description: dark photon mass (m_{Z_d}) and kinetic mixing angle (ε). The effective coupling of the dark photon to SM particles is the same as that of the photon but is suppressed by ε.

Figure 1 shows the dark photon parameter space (in the $m_{Z_d} - \varepsilon^2$ plane) along with the constraints from the electron and muon anomalous magnetic moments. These bounds are more robust compared to most other constraints, such as those from dilepton bump searches from Z_d decays, in the sense that they do not depend on the assumed decay branching ratios of the dark photon.

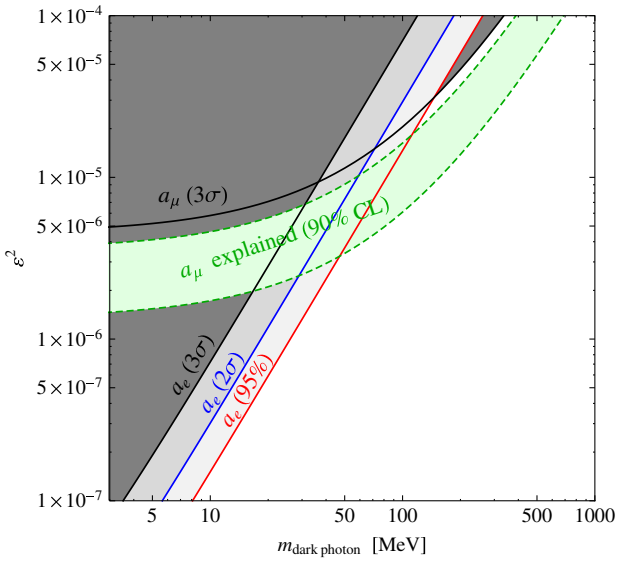

FIG. 1 (color online). Dark photon parameter space with bounds that are independent of the dark photon decay branching ratio. The green band is the region within which the 3.6σ deviation in a_μ can be explained by the dark photon (90% C.L.). The three a_e curves represent 3σ, 2σ, and 95%-C.L. bounds.

The muon anomalous magnetic moment theory and experiment exhibit a 3.6σ discrepancy [1]

$$\Delta a_\mu = a_\mu^{\text{exp}} - a_\mu^{\text{SM}} = 288(80) \times 10^{-11}, \tag{4}$$

with a slight change in the last digit made from a recent improved QED calculation [9], Higgs mass of 126 GeV [10,11], and a small change in the experimental value [1]. The long-standing discrepancy could be an early hint of new physics [12], assumed here to be the Z_d.

A one-loop contribution of the dark photon to the a_ℓ ($\ell = e, \mu$) [3,4,13,14] is given by

$$a_\ell^{Z_d} = \frac{\alpha}{2\pi}\varepsilon^2 F_V(m_{Z_d}/m_\ell) \tag{5}$$

$$F_V(x) \equiv \int_0^1 dz \frac{2z(1-z)^2}{(1-z)^2 + x^2 z}, \qquad F_V(0) = 1. \tag{6}$$

The parameter region of the dark photon that accommodates the a_μ deviation, using the fine-structure constant $\alpha = 1/137.036$, is indicated by the green band (90% C.L.) in Fig. 1. That figure also contains the a_μ bound at 3σ C.L. and a_e bounds at 3σ, 2σ, and 1.64σ (95% as it is one sided) C.L. using the constraint

$$\Delta a_e = -1.05(0.82) \times 10^{-12} \tag{7}$$

of Ref. [9]. The Δa_e value was significantly improved recently [15–17] by updates in the value of α and improvements in theory [9,18]. In the subsequent plots, we employ only the 2σ bound on a_e.

There are additional bounds on the dark photon parameters from various experiments (Fig. 2). They include beam dump experiments [19], rare meson decays (Υ decays at *BABAR* [20], ϕ decays at KLOE [21], π^0 decays at SINDRUM [22,23], WASA-at-COSY [24], HADES [25], η decays at HADES [25]), and fixed target experiments (MAMI [26], APEX [27]). There are also preliminary bounds from KLOE 2012 for the high mass region ($m_{Z_d} > 600$ MeV) [28] and the PHENIX experiment at BNL RHIC (π^0 decays) [29].

Furthermore, there are ongoing and proposed experiments to test the remaining green band and other parameter space. CERN NA48/2 experimental data (Dalitz decays of π^0 from $K^\pm \to \pi^\pm \pi^0$) are under analysis, and their sensitivity can cover $\varepsilon^2 \gtrsim$ several $\times 10^{-7}$ [30]. There are direct dark photon searches which use an electron beam with a fixed target of typically high atomic number [20] to produce Z_ds. The radiated dark photon can decay into a dilepton forming a resonance over the smooth SM off-shell photon background ($\gamma^* \to e^+e^-$). At Mainz, MAMI 2012–2013 experimental data are under analysis [31]. At Jefferson Lab (JLab) in Virginia, there are three proposed or approved searches for the dark photon (APEX, HPS, DarkLight) [32] using fixed target experiments.

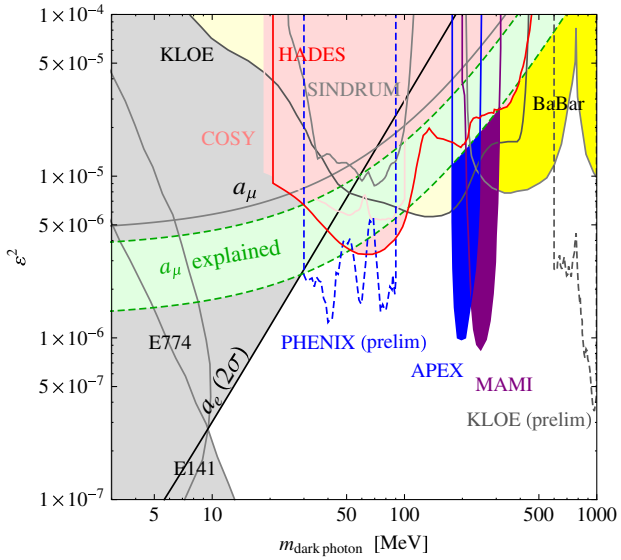

FIG. 2 (color online). Present bounds from various experiments on the dark photon parameter space. Some of these were obtained with the assumption of $\mathrm{BR}(Z_d \to \ell^+\ell^-) = 1$.

Similar searches have also been proposed using the VEPP-3 facility [33] at the Budker Institute in Russia. For a recent discussion of the signal and background estimation in the fixed target experiments, see Ref. [34].

Figure 2 shows the currently available bounds on the dark photon parameter space from the aforementioned experiments for a typical mass range of $m_{Z_d} \approx$ few MeV – GeV. (For an overview and overall constraints for wider ranges of parameter space, see Refs. [5,35]). Most of these bounds depend on the dark photon decay branching ratios and generally assume

$$\mathrm{BR}(Z_d \to \ell^+\ell^-) \equiv \mathrm{BR}(e^+e^-) + \mathrm{BR}(\mu^+\mu^-) = 1 \quad (8)$$

for $m_{Z_d} \lesssim 300$ MeV. The current published constraints, including a 2σ bound from Δa_e, only allow a rather tightly constrained parameter region in the green band: $m_{Z_d} \sim$ 30–50 MeV and $\varepsilon^2 \sim (2-4)\times 10^{-6}$. Most of this region is covered if we include preliminary bounds from the PHENIX experiment [29]. Note that the Δa_e bound is expected to improve with ongoing or planned efforts in the measurement of both a_e and α [36], which are independent of the Z_d decay branching ratio. In short, nearly the entire green band that can explain the a_μ deviation is already excluded or is under close scrutiny by various experiments, as is clear from Fig. 2.

Many of the constraints in Fig. 2 assume Z_d decays into an observable $\ell^+\ell^-$ pair with invariant mass m_{Z_d} and branching ratio ~1. If, instead, the Z_d decays primarily into invisible light particles (e.g. a pair of dark matter particles with mass $< m_{Z_d}/2$), that change would essentially negate all the bounds in Fig. 2, except those coming from anomalous magnetic moments. For the case of light dark matter coupled to Z_d with strength $q_{d\text{light}}\, g_d$, where $q_{d\text{light}}$ is its $U(1)_d$ charge and g_d is the gauge coupling, $Z_d \to$ light "invisible" matter will be dominant for $|q_{d\text{light}} g_d| \gtrsim \varepsilon e$, which for the region in ε we subsequently consider $|\varepsilon| \sim 2\times 10^{-3}$ suggests (with $\alpha_d = g_d^2/4\pi$)

$$3\times 10^{-8} \lesssim q_{d\text{light}}^2 \alpha_d \lesssim 10^{-2} \quad (9)$$

as an interesting range for discussion. The upper bound in that range is somewhat arbitrary but is appropriate for the models we subsequently consider. We do note, however, that for larger $q_{d\text{light}}^2 \alpha_d \sim 0.1$ experimental constraints from beam dump experiments [37,38] are already providing interesting bounds. They effectively assume Z_d boson production ($\sim\varepsilon^2\alpha$) followed by Z_d decay and subsequent detection of the Z_d decay products. So, even for a primary $Z_d \to$ light dark matter scenario, detection is possible if $q_{d\text{light}} g_d$ is relatively large. Under those circumstances, they are likely to rule out much of the Δa_μ discrepancy band. (For examples of future beam dump experiments designed to search for light dark matter, see Refs. [39–42].)

Instead of explaining constraints from beam dump experiments, which is beyond the scope of this paper, we next concentrate on the decay $K^\pm \to \pi^\pm Z_d$, $Z_d \to$ light dark matter which is insensitive to the value of $q_{d\text{light}}^2 \alpha_d$ as long as it falls in the range of Eq. (9).

III. DARK KAON DECAYS

As seen in the previous section, flavor-conserving meson decays provide strong constraints on dark photon phenomenology. We now consider the impact of flavor-changing kaon decays on dark photon parameters. Earlier discussions about Z_d implications for meson decays in various contexts can be found in the literature [4,43–49].

From the formalism given in the Appendix, the rate for $K^\pm \to \pi^\pm Z_d$, assuming a kinetically mixed dark photon, is given by

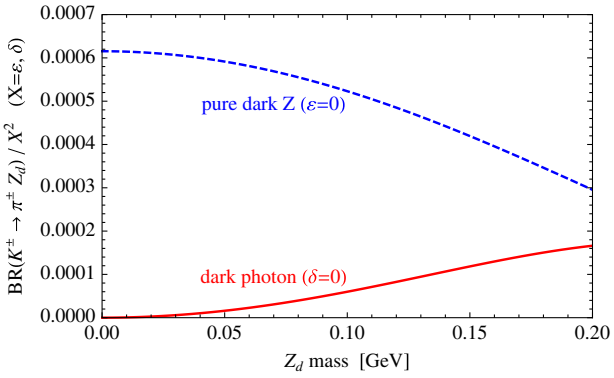

FIG. 3 (color online). $\mathrm{BR}(K^\pm \to \pi^\pm Z_d)$ in the dark photon limit ($\delta = 0$, solid line) and the pure dark Z limit ($\varepsilon = 0$, dashed line), as a function of m_{Z_d} for both ε (dark photon) and δ (pure dark Z). Here, $m_{H^\pm} = 160$ GeV is assumed.

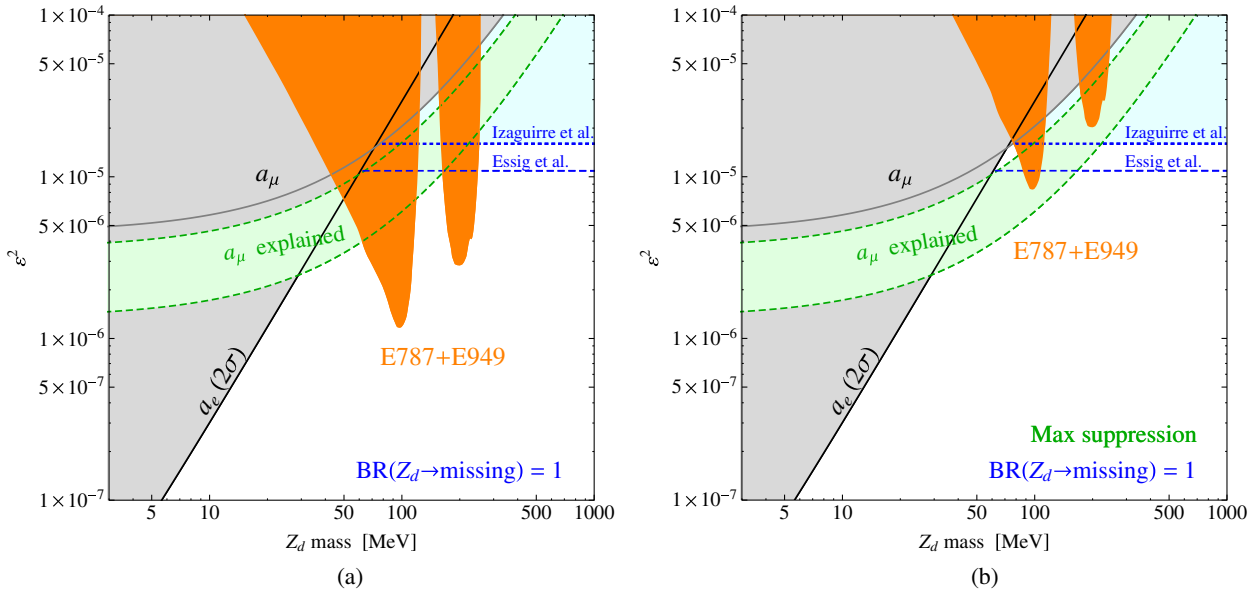

FIG. 4 (color online). Constraints from BNL E787+E949 experiments ($K \to \pi +$ nothing), at 95% C.L., on the dark photon parameter space (dark orange shaded area covered by E787+E949) for BR($Z_d \to$ missing) $= 1$ for (a) dark photon and (b) dark Z with maximum suppression. Also illustrated are constraints from $e^+e^- \to \gamma +$ invisible based on *BABAR* data as given in Ref. [41] by Izaguirre *et al.* and Ref. [51] by Essig *et al.*

$$\Gamma(K^\pm \to \pi^\pm Z_d)|_\varepsilon = \frac{\varepsilon^2 \alpha W^2 m_{Z_d}^2}{2^{10}\pi^4} \frac{\sqrt{\lambda(m_K^2, m_\pi^2, m_{Z_d}^2)}}{m_K^7} \times [(m_K^2 - m_\pi^2)^2 - m_{Z_d}^2(2m_K^2 + 2m_\pi^2 - m_{Z_d}^2)], \tag{10}$$

which is consistent with the results in Ref. [4]. The function W [50] is approximately given by $W^2 \approx 3 \times 10^{-12}(1 + 2m_{Z_d}^2/m_K^2)$ [4,51]. This process is suppressed for small m_{Z_d} and $m_{Z_d} \simeq m_K - m_\pi$ (the end of phase space). The branching ratio associated with the rate in Eq. (10) is presented in Fig. 3 by the solid curve, as a function of m_{Z_d}.

Equation (10) and the uncertainties of the experimentally measured branching ratios of $K^\pm \to \pi^\pm \ell^+\ell^-$ [1,52,53] roughly yield for $Z_d \to \ell^+\ell^-$

$$\varepsilon^2 \lesssim \frac{10^{-4}}{\mathrm{BR}(Z_d \to \ell^+\ell^-)} \left(\frac{100\ \mathrm{MeV}}{m_{Z_d}}\right)^2. \tag{11}$$

This result does not give significant constraints over the existing bounds of $\varepsilon^2 \lesssim 10^{-5}$ in the parameter region of interest $m_{Z_d} \lesssim 300$ MeV (cf. Fig. 2), for typically assumed BR($Z_d \to \ell^+\ell^-$) $= 1$. The situation gets worse if Z_d decays primarily into very light dark matter or other invisible particles dominantly, lowering BR($Z_d \to \ell^+\ell^-$).

The BNL E949 experiment combined with E787 results [54] measured the illusive $K^+ \to \pi^+\nu\bar{\nu}$ and gave upper bounds on the BR($K^+ \to \pi^+ Z_d$) as a function of the Z_d mass, for $Z_d \to$ "missing energy." The region around $m_{ee} \sim 140$ MeV is not constrained, corresponding to events that were vetoed to avoid the large background from $K^+ \to \pi^+\pi^0$.

Figure 4(a) shows the resulting constraints of this "$K \to \pi +$ nothing" search on the dark photon model for BR($Z_d \to$ missing) $= 1$, but scaling to 95% C.L., using Eq. (10). Rather large areas in the a_μ-favored green band are excluded, i.e., the orange shaded regions around $m_{Z_d} \sim 100$, 200 MeV. The dotted and dashed lines correspond to the constraints from $e^+e^- \to \gamma +$ invisible, adapted from Refs. [41] and [51], respectively, based on *BABAR* results [55].

We see that these bounds together eliminate much of the a_μ band, leaving only small regions of parameter space to accommodate the $g_\mu - 2$ discrepancy.

The CERN NA62 [56] and the proposed Fermilab ORKA experiments [57] (precision measurements of $K \to \pi +$ nothing and other rare K decays) increase the $K \to \pi Z_d$ sensitivity by at least an order of magnitude, and the kaon decay exclusion curves in Fig. 4 may be accordingly lowered.

IV. DARK Z AND $Z - Z_d$ MASS MIXING

While the dark photon, whose coupling is mainly proportional to the electromagnetic coupling, can be realized using a relatively simple mechanism for the Z_d mass (a condensing scalar Higgs singlet or Stueckelberg mechanism [58]), a more general Higgs sector—for instance, a two Higgs doublet model (2HDM)—could lead to mass mixing of Z_d with the SM Z [47]. In this expanded framework, the interaction Lagrangian of the Z_d with the SM fermions includes both $\gamma - Z_d$ mixing as well as $Z - Z_d$ mixing

$$\mathcal{L}_{\text{dark } Z} = -\left(\varepsilon e J^{\mu}_{em} + \varepsilon_Z \frac{g}{2\cos\theta_W} J^{\mu}_{NC}\right) Z_{d\mu}, \tag{12}$$

where

$$J^{\mu}_{NC} \equiv (T_{3f} - 2Q_f \sin^2\theta_W)\bar{f}\gamma^{\mu} f - T_{3f}\bar{f}\gamma^{\mu}\gamma_5 f \tag{13}$$

is the weak neutral current and $T_{3f} = \pm 1/2$ [47]. An additional parameter ε_Z is present to describe the $Z - Z_d$ mixing. In this case, the vector state Z_d is dubbed a "dark Z" to emphasize that it also has Z-like couplings.

In the dark Z model, there are three independent parameters needed to describe the phenomenology: the dark Z mass m_{Z_d}, kinetic mixing parameter ε, and the $Z - Z_d$ mass mixing parameter ε_Z. Thus, the dark photon model can be viewed as a special case (the $\varepsilon_Z = 0$ limit) of a more general dark Z model. (We note that kinetic mixing will yield $\varepsilon_Z \sim \varepsilon m^2_{Z_d}/m^2_Z$. We do not consider that small effect, for $m_{Z_d} < 1$ GeV, here.)

The $Z - Z_d$ mixing gives rise to interesting phenomenological features, such as providing a new low mass mediator of parity violation, that are typically absent in the light dark photon models. Also, at energies large compared to m_{Z_d}, the longitudinally polarized Z_d dominates and has an enhanced coupling of order $(E/m_{Z_d})\varepsilon_Z$ (for $E \gtrsim m_{Z_d}$). The Goldstone boson equivalence theorem [59] implies that the longitudinal dark Z mode at high energies exhibits properties similar to an axion, and one can use computations involving the latter to estimate the rates for processes associated with the former [47].

The $Z - Z_d$ mass mixing parameter ε_Z in Eq. (12) is further parametrized by

$$\varepsilon_Z \equiv \frac{m_{Z_d}}{m_Z}\delta, \tag{14}$$

and the mass-squared matrix (in the $\varepsilon = 0$ limit) can be written as

$$M^2_{ZZ_d} \simeq \begin{pmatrix} m^2_Z & -\delta m_Z m_{Z_d} \\ -\delta m_Z m_{Z_d} & m^2_{Z_d} \end{pmatrix} \tag{15}$$

for $m^2_{Z_d} \ll m^2_Z$. For more details about the formalism, see Ref. [47].

The bounds on δ come from various experiments, including low-energy parity violation, Higgs decays, and flavor-changing rare meson decays. The typical bounds are $|\delta| \lesssim 10^{-2}$–$10^{-3}$, depending on the mass and decay branching ratio of Z_d [47]. The low momentum transfer (Q) parity violation experiments provide significant constraints on the parameter space, as the effect vanishes for $Q^2 \gg m^2_{Z_d}$. They include atomic parity violation and polarized electron-scattering experiments [47,60].

The dark Z model opens a new window into the dark sector through the Higgs boson at the LHC experiments [47,61,62]. Unlike the simple dark photon model, the dark Z leads to a small but potentially measurable $H \to ZZ_d$ decay, which is from the SM $H \to ZZ$ process with a Z replaced with Z_d through $Z - Z_d$ mixing. Because of the small Z_d mass, it is an on-shell decay process producing a boosted Z_d with the aforementioned enhancement for longitudinal polarization. The recently discovered SM-like Higgs boson [10,11] provides a constraint on the dark Z boson. The charged Higgs boson—from a 2HDM realization of dark Z—may escape current LHC searches, as it can dominantly decay into Z_d final states as WZ_d [63] or WZ_dZ_d [61] depending on the masses of the non-SM-like scalars. For a detailed quantitative study, see Ref. [64].

V. RARE KAON DECAYS IN THE PRESENCE OF $Z - Z_d$ MASS MIXING

We now revisit the $K^{\pm} \to \pi^{\pm} Z_d$ decay in the dark Z model. This process was discussed in Ref. [47] with the Z_d replaced by an axion, which is possible for the longitudinally polarized Z_d (Goldstone equivalence theorem). Here we employ a similar but more comprehensive approach. We take a coupling adapted from the axion approximation ($\propto \varepsilon_Z$), along with that from kinetic mixing ($\propto \varepsilon$), so that we can describe both interactions and their interference effects. The formalism for $K^{\pm} \to \pi^{\pm} Z_d$ is given in the Appendix, where more details are provided.

The more general decay width for $K^{\pm} \to \pi^{\pm} Z_d$ is given by

$$\Gamma(K^{\pm} \to \pi^{\pm} Z_d) = \Gamma(K^{\pm} \to \pi^{\pm} Z_d)|_{\varepsilon} \left| 1 \pm \frac{\delta B}{\varepsilon A m_{Z_d} m_Z} \right|^2, \tag{16}$$

with A and B given in the Appendix. As discussed in the Appendix, A has been assumed to be real, but a $\pm$ sign arbitrariness has been included to reflect uncertainty in the long-distance amplitude sign of A.

In the pure dark Z limit ($\varepsilon = 0$), we get

$$\begin{aligned} \Gamma(K^{\pm} \to \pi^{\pm} Z_d)|_{\varepsilon_Z} = {} & \frac{g^6 |U^*_{td} U_{ts}|^2}{2^{20}\pi^5} (f_+)^2 X_1^2 \delta^2 \\ & \times \frac{m_t^4}{m_W^6 m_K^3} \sqrt{\lambda(m_K^2, m_\pi^2, m^2_{Z_d})} \\ & \times [(m_K^2 - m_\pi^2)^2 - m^2_{Z_d} \\ & \times (2m_K^2 + 2m_\pi^2 - m^2_{Z_d})], \end{aligned} \tag{17}$$

where X_1 [65,66] depends on the charged Higgs mass and top mass and is plotted in Fig. 5. Note that the above rate does not vanish as $m_{Z_d} \to 0$. The suppression for small m_{Z_d} in the dark photon model does not necessarily occur in the dark Z model.

The dashed curve in Fig. 3 represents $\text{BR}(K^{\pm} \to \pi^{\pm} Z_d)|_{\varepsilon_Z}$, with $f_+ \simeq 1$. This plot agrees with the result

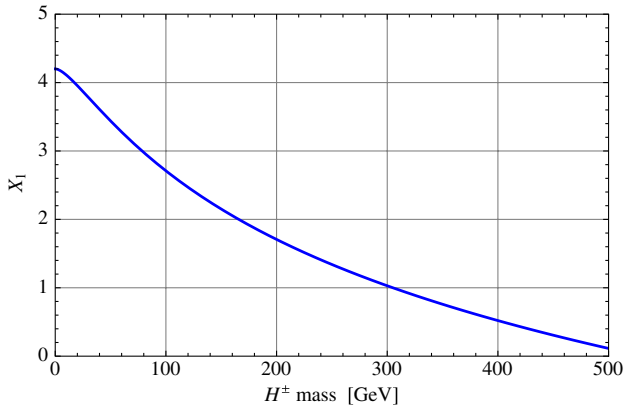

FIG. 5 (color online). X_1 [65,66] as a function of the charged Higgs mass with $m_t = 163$ GeV.

in Ref. [47], which takes $m_{H^\pm} = 150$ GeV and includes the small charm quark contribution, leading to a strong constraint $\delta \lesssim 10^{-3}$ (except for a region near $m_{Z_d} \sim m_\pi$).

A cancellation may occur between kinetic mixing (ε term) and $Z - Z_d$ mass mixing (δ term). In that way, the dark Z may be able to evade the $K \to \pi +$ nothing search constraints. While A is taken to be real, B is complex due to $U_{td}^* U_{ts} \simeq -(3.36 + 1.35i) \times 10^{-4}$, and there can be a cancellation between the A and the real part of B. A complete cancellation is impossible because $\mathrm{Im}[B] \neq 0$ and its contribution to $\mathrm{BR}(K^\pm \to \pi^\pm Z_d)$ must be smaller than the experimental bound given in Ref. [54].

Figure 4(b) shows the maximum suppression of the $K \to \pi +$ nothing constraint, which can be shown to be $1.35^2/(3.36^2 + 1.35^2) \simeq 1/7$. This corresponds to

$$\delta = \mp\varepsilon \frac{A m_{Z_d} m_Z \mathrm{Re}[B]}{|B|^2} \simeq \pm\varepsilon(6.2)\frac{(m_{Z_d}/\mathrm{GeV})}{X_1} \quad (18)$$

for a given X_1 value (depending on $m_{H^\pm}$). It is interesting to observe that constraints on ε and δ are both alleviated for the destructive interference requirement.

VI. RUNNING OF THE WEAK MIXING ANGLE

In this section, we consider what type of experiments can still test the dark Z when the searches for dilepton bump or missing energy (especially, $K \to \pi +$ nothing search) miss the signals due to the destructive interference effect discussed in the previous section.

The dark Z can still modify neutral current phenomenology in the low Q (momentum transfer) regime [47]. The effective value of the weak mixing angle is modified for $Q \lesssim m_{Z_d}$, which leaves the dark Z parity violating effect still visible in low-energy experiments. As suggested in Refs. [47,60], low Q^2 polarized electron-scattering experiments in progress or proposed at various facilities (including JLab and MAMI at Mainz) are excellent probes of this kind of low-energy new physics if $Q^2 \lesssim m_{Z_d}^2$. Another type of low-energy test is atomic parity violation [67], which requires precise understanding of the heavy atom physics.

The weak mixing angle shift by the dark Z is given in Refs. [47,60] as

$$\Delta \sin^2\theta_W(Q^2) = -\varepsilon\delta \frac{m_Z}{m_{Z_d}} \sin\theta_W \cos\theta_W f(Q^2/m_{Z_d}^2), \quad (20)$$

with $f(Q^2/m_{Z_d}^2) = 1/(1 + Q^2/m_{Z_d}^2)$ (for polarized electron-scattering experiments) and $f(Q^2/m_{Z_d}^2) \sim 1$ (for atomic parity violation of a heavy atom [68]). We use $\sin^2\theta_W = 0.238$, appropriate for low-energy physics.

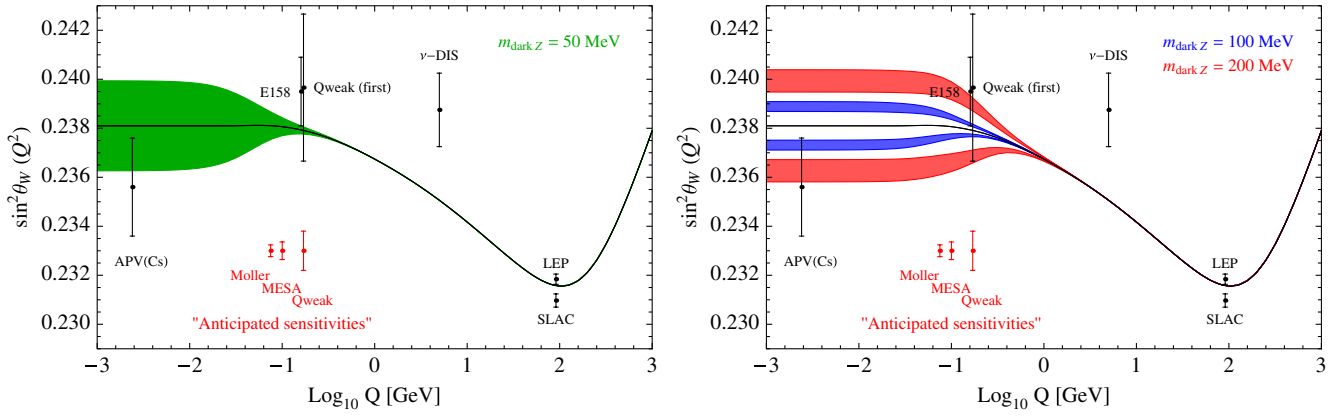

(a) (b)

FIG. 6 (color online). Running of the effective weak mixing angle, $\sin^2\theta_W(Q^2)$ with energy scale Q. The solid (black) curve is the SM prediction, and the shaded regions are predictions with a dark Z for given masses (a) $m_{Z_d} = 50$ MeV and (b) $m_{Z_d} = 100, 200$ MeV with ε^2 from the a_μ green band in Fig. 1. BNL kaon decay constraints are applied. The red points and their error bars represent, respectively, the average Q and the anticipated sensitivities for JLab Moller, Mainz MESA (P2), and JLab Qweak. The results depend on the charged Higgs mass, and $m_{H^\pm} = 160$ GeV is used.

A convenient way to illustrate the effect of quantum corrections to $\gamma - Z$ mixing is via the running of $\sin^2\theta_W(Q^2)$ introduced in Ref. [69]. It describes the evolution at low energy primarily through quark loops (but with some small lepton effects) and then hits a minimum when W^+W^- loops effectively change the sign of the evolution slope at high $Q^2 > 2m_W$. That SM plot will be modified at low Q^2 by the dark Z shift given in Eq. (20). To illustrate the effect, we give in Fig. 6 modifications of the low Q^2 dark Z effect for specific values of $m_{Z_d} = 50$, 100, and 200 MeV. Definite nonzero correction bands are predicted for $m_{Z_d} = 100$, 200 MeV assuming that the dark Z solves the $g_\mu - 2$ discrepancy and satisfies the bounds in Fig. 4.

The shaded regions (potential deviation of weak mixing angle) clearly show that the effect of the dark Z is visible for $Q \lesssim m_{Z_d}$. The two branches of each curve correspond to a potential sign ambiguity of $\varepsilon\delta$ in Eq. (20) that could result from QCD effects in the relative sign between A and $\mathrm{Re}[B]$. In principle, this sign, required for the cancellation between the two amplitudes, may be determined through a detailed analysis of QCD corrections to the amplitudes. However, such a study is outside the scope of this paper. We simply plot both possibilities to show the form of the expected effects in each case.

There are ongoing or planned low-energy polarized electron-scattering experiments, including JLab Qweak (ep) [70], JLab Moller (ee) [71], and MESA P2 (ep) [72]. For recent reviews on the low-energy weak mixing angle measurements, see Refs. [73,74]. As is clear from the sensitivities indicated in Fig. 6, a deviation in the weak mixing angle by dark Z can be large enough to be tested by these low-energy parity measurements. Furthermore, using the difference in average momentum transfer (Q) of these experiments, including the atomic parity violation, it may be possible to fit the data to constrain the mass and couplings of Z_d if deviations from the SM predictions arise.

VII. SUMMARY AND CONCLUSIONS

In this paper, we examined the properties of a hypothetical dark photon (or dark Z), which was proposed to address various astrophysical anomalies and the deviation in the muon anomalous magnetic moment. We discussed current bounds and near future sensitivity, including a detailed discussion of implications from the electron anomalous magnetic moment.

We also considered scenarios in which the dark photon decays primarily into light dark matter or other invisible particles, where the typical searches assuming $\mathrm{BR}(Z_d \to \ell^+\ell^-) = 1$ would not be sensitive to the signal. This case is timely as the current experiments based on bump searches in addition to the electron and muon anomalous magnetic moment are tending to exclude most of the preferred ε parameter region that can explain the 3.6σ muon $g-2$ discrepancy. Considering that there are active analysis of existing data and numerous future experiments, as partly discussed in Sec. II, it is expected that the whole region will be tested soon and possibly ruled out. Of course, a more interesting outcome would be discovery of the dark sector.

Interestingly, the $K \to \pi+$ nothing searches (BNL E787+ E949) can exclude the scenario of dominant Z_d decay into invisible particles in large parts of the dark photon parameter space. Used in conjunction with recent bounds from $e^+e^- \to \gamma+$ missing energy [41,51] (based on *BABAR* results [55]), one can significantly constrain the $g_\mu - 2$ preferred ε parameter space. We emphasized that for the dark Z, which is essentially a dark photon with a more general coupling, we can potentially evade the current rare kaon decay constraints on missing energy searches due to the possibility of a cancellation between the kinetic mixing and $Z - Z_d$ mass mixing. As the light Z_d contribution to the muon anomalous magnetic moment is independent of its decay branching ratio, the Z_d can still remain as the solution to the muon anomaly. In this case, low-energy polarized electron scattering as well as atomic parity violation predictions can provide sensitive tests of that scenario.

ACKNOWLEDGMENTS

We thank R. Essig for discussions. This work was supported in part by the U.S. DOE under Grants No. DE-AC02-98CH10886 and No. DE-AC05-06OR23177 and by the NSF under Grant No. PHY-1068008. W. M. acknowledges partial support as a Fellow in the Gutenberg Research College. H. L. appreciates hospitality during his visit to BNL.

APPENDIX: FORMALISM

The amplitude for $K^+(k) \to \pi^+(p) + Z_d(q)$ is given by

$$\begin{aligned}\mathcal{M}(K^+ \to \pi^+ Z_d) &= (\varepsilon A\langle\pi^+(p)|q^2\bar{s}_L\gamma_\mu d_L - q_\mu q^\nu \bar{s}_L\gamma_\nu d_L|K^+(k)\rangle \\ &\quad \pm\delta\frac{m_{Z_d}}{m_Z}B\langle\pi^+(p)|\bar{s}_L\gamma_\mu d_L|K^+(k)\rangle)\epsilon^{*\mu}(q) \qquad \text{(A1)}\\ &= \frac{1}{2}f_+(q^2)\left(\varepsilon m_{Z_d}^2 A \pm \delta\frac{m_{Z_d}}{m_Z}B\right)(k+p)_\mu\epsilon^{*\mu}(q), \qquad \text{(A2)}\end{aligned}$$

where we have used $\epsilon^\mu(q)q_\mu = 0$ and the hadronic matrix elements

$$\langle\pi^+(p)|\bar{s}\gamma_\mu d|K^+(k)\rangle = f_+(q^2)(k+p)_\mu, \qquad \text{(A3)}$$

$$\langle\pi^+(p)|\bar{s}\gamma_\mu\gamma_5 d|K^+(k)\rangle = 0, \qquad \text{(A4)}$$

with $|f_+(0)| = 1$. We have allowed for a $\pm$ arbitrariness in the relative sign of A and B because A is dependent on

long-distance QCD effects that could change its sign. We also assume that A is real in our discussion. In principle, it could have an imaginary part. We avoid that issue by focusing on $m_{Z_d} < 2m_\pi$ since imaginary parts are due primarily to a two-pion intermediate state in the chiral expansion [50]. Taking the formalism introduced in Ref. [4] (for A) and Refs. [65,66] (for B), we have

$$A = \frac{1}{(4\pi)^2}\frac{eW}{m_K^2(f_+/2)}, \tag{A5}$$

$$B = \frac{1}{(4\pi)^2}\frac{g^3 m_t^2 m_Z}{8m_W^3}(U_{td}^* U_{ts})X_1, \tag{A6}$$

where we have included only a dominant top quark loop term in B. (For an approach based on the SM-loop-induced photon and Z couplings, see Ref. [75].) The dark photon case corresponds to $\delta = 0$, and the pure dark Z limit is obtained for $\varepsilon = 0$. The function W is given in Ref. [50]. It was approximated by $W^2 \approx 3 \times 10^{-12}(1 + 2q^2/m_K^2)$ [4,51]. For W/f_+, we use $\pm 1.73 \times 10^{-6}$ where a sign arbitrariness is allowed. The function X_1 [65,66], plotted in Fig. 5, depends on the charged Higgs mass and top mass, for which we use $m_t = 163$ GeV (the QCD corrected value in the $\overline{\text{MS}}$ scheme).

The decay width for $K^+ \to \pi^+ + Z_d$ is then

$$\Gamma(K^+ \to \pi^+ Z_d) = 4\pi\frac{\sqrt{\lambda(m_K^2, m_\pi^2, m_{Z_d}^2)}}{64\pi^2 m_K^3}\sum_{\text{pol}}|\mathcal{M}|^2, \tag{A7}$$

with $\lambda(x, y, z) \equiv x^2 + y^2 + z^2 - 2xy - 2yz - 2zx$ and the amplitude squared written as

$$\sum_{\text{pol}}|\mathcal{M}|^2 = \frac{1}{4}(f_+)^2\left[\left(\frac{m_K^2 - m_\pi^2}{m_{Z_d}}\right)^2 - (2m_K^2 + 2m_\pi^2 - m_{Z_d}^2)\right] \times \left|\varepsilon m_{Z_d}^2 A \pm \delta\frac{m_{Z_d}}{m_Z}B\right|^2. \tag{A8}$$

[1] J. Beringer *et al.* (Particle Data Group Collaboration), Phys. Rev. D **86**, 010001 (2012) and 2013 partial update for the 2014 edition (http://pdg.lbl.gov).
[2] For instances, see N. Arkani-Hamed, D. P. Finkbeiner, T. R. Slatyer, and N. Weiner, Phys. Rev. D **79**, 015014 (2009); C. Boehm, D. Hooper, J. Silk, M. Casse, and J. Paul, Phys. Rev. Lett. **92**, 101301 (2004); P. Fayet, Phys. Rev. D **70**, 023514 (2004).
[3] For early work on the contribution of a light $U(1)$ gauge boson to $g_\mu - 2$, using direct rather than mixing-induced couplings to fermions, see, for example, P. Fayet, Nucl. Phys. **B187**, 184 (1981); S. N. Gninenko and N. V. Krasnikov, Phys. Lett. B **513**, 119 (2001); and P. Fayet, Phys. Rev. D **75**, 115017 (2007).
[4] M. Pospelov, Phys. Rev. D **80**, 095002 (2009).
[5] R. Essig, J. A. Jaros, W. Wester, P. H. Adrian, S. Andreas, T. Averett, O. Baker, and B. Batell *et al.*, arXiv:1311.0029.
[6] L. A. Anchordoqui, H. Goldberg, and G. Steigman, Phys. Lett. B **718**, 1162 (2013).
[7] S. Weinberg, Phys. Rev. Lett. **110**, 241301 (2013).
[8] B. Holdom, Phys. Lett. B **166**, 196 (1986).
[9] T. Aoyama, M. Hayakawa, T. Kinoshita, and M. Nio, Phys. Rev. Lett. **109**, 111807 (2012).
[10] ATLAS Collaboration, Report No. ATLAS-CONF-2013-012.
[11] CMS Collaboration, Report No. CMS-PAS-HIG-13-001.
[12] A. Czarnecki and W. J. Marciano, Phys. Rev. D **64**, 013014 (2001).
[13] H. Davoudiasl, R. Kitano, G. D. Kribs, and H. Murayama, Phys. Rev. D **71**, 113004 (2005).
[14] J. P. Leveille, Nucl. Phys. **B137**, 63 (1978).
[15] H. Davoudiasl, H.-S. Lee, and W. J. Marciano, Phys. Rev. D **86**, 095009 (2012).
[16] M. Endo, K. Hamaguchi, and G. Mishima, Phys. Rev. D **86**, 095029 (2012).
[17] D. Hanneke, S. Fogwell, and G. Gabrielse, Phys. Rev. Lett. **100**, 120801 (2008).
[18] R. Bouchendira, P. Clade, S. Guellati-Khelifa, F. Nez, and F. Biraben, Phys. Rev. Lett. **106**, 080801 (2011).
[19] S. Andreas, C. Niebuhr, and A. Ringwald, Phys. Rev. D **86**, 095019 (2012).
[20] J. D. Bjorken, R. Essig, P. Schuster, and N. Toro, Phys. Rev. D **80**, 075018 (2009).
[21] D. Babusci *et al.* (KLOE-2 Collaboration), Phys. Lett. B **720**, 111 (2013).
[22] R. Meijer Drees *et al.* (SINDRUM I Collaboration), Phys. Rev. Lett. **68**, 3845 (1992).
[23] S. N. Gninenko, Phys. Rev. D **87**, 035030 (2013).
[24] P. Adlarson *et al.* (WASA-at-COSY Collaboration), Phys. Lett. B **726**, 187 (2013).
[25] G. Agakishiev *et al.* (HADES Collaboration), arXiv: 1311.0216.
[26] H. Merkel *et al.* (A1 Collaboration), Phys. Rev. Lett. **106**, 251802 (2011).
[27] S. Abrahamyan *et al.* (APEX Collaboration), Phys. Rev. Lett. **107**, 191804 (2011).
[28] F. Curciarello (KLOE/KLOE2 Collaboration), J. Phys. Conf. Ser. **424**, 012006 (2013).
[29] Y. Yamaguchi (PHENIX Collaboration), "A Search for Beyond the Standard Model Particles with the PHENIX Detector at RHIC," DNP 2013 Meeting.

[30] M. J. Amaryan, M. Bashkanov, M. Benayoun, F. Bergmann, J. Bijnens, L. C. Balkestahl, H. Clement, and G. Colangelo *et al.*, arXiv:1308.2575.

[31] T. Beranek, H. Merkel, and M. Vanderhaeghen, Phys. Rev. D **88**, 015032 (2013).

[32] J. Dudek, R. Ent, R. Essig, K. Kumar, C. Meyer, R. McKeown, Z. E. Meziani, and G. A. Miller *et al.*, Eur. Phys. J. A **48**, 187 (2012).

[33] B. Wojtsekhowski, D. Nikolenko, and I. Rachek, arXiv: 1207.5089.

[34] T. Beranek and M. Vanderhaeghen, Phys. Rev. D **89**, 055006 (2014).

[35] J. Jaeckel, Frascati Phys. Ser. **56**, 172 (2012).

[36] G. F. Giudice, P. Paradisi, and M. Passera, J. High Energy Phys. 11 (2012) 113.

[37] M. D. Diamond and P. Schuster, Phys. Rev. Lett. **111**, 221803 (2013).

[38] B. Batell, R. Essig, and Z. Surujon, work in progress.

[39] B. Batell, M. Pospelov, and A. Ritz, Phys. Rev. D **80**, 095024 (2009).

[40] R. Dharmapalan *et al.* (MiniBooNE Collaboration), arXiv: 1211.2258.

[41] E. Izaguirre, G. Krnjaic, P. Schuster, and N. Toro, Phys. Rev. D **88**, 114015 (2013).

[42] S. Andreas, S.V. Donskov, P. Crivelli, A. Gardikiotis, S. N. Gninenko, N. A. Golubev, F. F. Guber, A. P. Ivashkin, *et al.*, arXiv:1312.3309.

[43] P. Fayet, Phys. Rev. D **74**, 054034 (2006).

[44] Y. Kahn, M. Schmitt, and T. M. P. Tait, Phys. Rev. D **78**, 115002 (2008).

[45] B. Batell, M. Pospelov, and A. Ritz, Phys. Rev. D **79**, 115008 (2009).

[46] V. Barger, C.-W. Chiang, W.-Y. Keung, and D. Marfatia, Phys. Rev. Lett. **108**, 081802 (2012).

[47] H. Davoudiasl, H.-S. Lee, and W. J. Marciano, Phys. Rev. D **85**, 115019 (2012).

[48] Y. Kahn and J. Thaler, Phys. Rev. D **86**, 115012 (2012).

[49] T. Beranek and M. Vanderhaeghen, Phys. Rev. D **87**, 015024 (2013).

[50] G. D'Ambrosio, G. Ecker, G. Isidori, and J. Portoles, J. High Energy Phys. 08 (1998) 004.

[51] R. Essig, J. Mardon, M. Papucci, T. Volansky, and Y.-M. Zhong, J. High Energy Phys. 11 (2013) 167.

[52] R. Appel *et al.* (E865 Collaboration), Phys. Rev. Lett. **83**, 4482 (1999).

[53] J. R. Batley *et al.* (NA48/2 Collaboration), Phys. Lett. B **677**, 246 (2009).

[54] A. V. Artamonov *et al.* (BNL-E949 Collaboration), Phys. Rev. D **79**, 092004 (2009).

[55] B. Aubert *et al.* (*BABAR* Collaboration), arXiv:0808.0017.

[56] G. Ruggiero (NA62 Collaboration), *Proc. Sci.* KAON2013, 032 (2013).

[57] E. T. Worcester (ORKA Collaboration), Nucl. Phys. B, Proc. Suppl. **233**, 285 (2012).

[58] For a review, see H. Ruegg and M. Ruiz-Altaba, Int. J. Mod. Phys. A **19**, 3265 (2004).

[59] J. M. Cornwall, D. N. Levin, and G. Tiktopoulos, Phys. Rev. D **10**, 1145 (1974); J. M. Cornwall, D. N. Levin, and G. Tiktopoulos, Phys. Rev. D **11**, 972(E) (1975); M. S. Chanowitz and M. K. Gaillard, Nucl. Phys. **B261**, 379 (1985); W. J. Marciano and S. S. D. Willenbrock, Phys. Rev. D **37**, 2509 (1988).

[60] H. Davoudiasl, H.-S. Lee, and W. J. Marciano, Phys. Rev. Lett. **109**, 031802 (2012).

[61] H.-S. Lee and M. Sher, Phys. Rev. D **87**, 115009 (2013).

[62] H. Davoudiasl, H.-S. Lee, I. Lewis, and W. J. Marciano, Phys. Rev. D **88**, 015022 (2013).

[63] H. Davoudiasl, W. J. Marciano, R. Ramos, and M. Sher, arXiv:1401.2164.

[64] K. Kong, H.-S. Lee, and M. Park, Phys. Rev. D **89**, 074007 (2014).

[65] L. J. Hall and M. B. Wise, Nucl. Phys. **B187**, 397 (1981).

[66] M. Freytsis, Z. Ligeti, and J. Thaler, Phys. Rev. D **81**, 034001 (2010).

[67] S. C. Bennett and C. E. Wieman, Phys. Rev. Lett. **82**, 2484 (1999); S. C. Bennett and C. E. Wieman, Phys. Rev. Lett.**82**, 4153(E) (1999); S. C. Bennett and C. E. Wieman, Phys. Rev. Lett.**83**, 889(E) (1999); S. L. Gilbert, M. C. Noecker, R. N. Watts, and C. E. Wieman, Phys. Rev. Lett. **55**, 2680 (1985).

[68] C. Bouchiat and P. Fayet, Phys. Lett. B **608**, 87 (2005); C. Bouchiat and C. A. Piketty, Phys. Lett. **128B**, 73 (1983).

[69] W. J. Marciano and A. Sirlin, Phys. Rev. Lett. **46**, 163 (1981); A. Czarnecki and W. J. Marciano, Phys. Rev. D **53**, 1066 (1996); Int. J. Mod. Phys. A **15**, 2365 (2000); A. Ferroglia, G. Ossola, and A. Sirlin, Eur. Phys. J. C **34**, 165 (2004).

[70] D. Androic *et al.* (Qweak Collaboration), Phys. Rev. Lett. **111**, 141803 (2013).

[71] The Moller Experiment, JLab Proposal E-12-09-005.

[72] K. Aulenbacher, Hyperfine Interact. **200**, 3 (2011); H. Spiesberger, Proceedings of DIS 2012.

[73] K. S. Kumar, S. Mantry, W. J. Marciano, and P. A. Souder, Annu. Rev. Nucl. Part. Sci. **63**, 237 (2013).

[74] J. Erler, C. J. Horowitz, S. Mantry, and P. A. Souder, arXiv:1401.6199.

[75] T. Inami and C. S. Lim, Prog. Theor. Phys. **65**, 297 (1981); T. Inami and C. S. Lim, Prog. Theor. Phys.**65**, 1772(E) (1981).